J. At. Mol. Sci.
doi: 10.4208/jams.021916.042616a

Vol. 7, No. 2, pp. 87-95
May 2016

Quasiclassical trajectory study of the stereodynamics for the Au + H_2 (v=0, j=0) $\rightarrow$ AuH + H reaction

Guanygan Sha[a], Dahai Cheng[b] and Changgong Meng[a,*]

[a] *Experimental Center of Chemistry, School of Chemistry, Dalian University of Technology, Dalian 116024, P. R. China*
[b] *School of Physics and Optoelectronic Technology, and College of Advanced Science and Technology, Dalian University of Technology, Dalian 116024, P. R. China*

Received 19 February 2016; Accepted (in revised version) 26 April 2016
Published Online 25 May 2016

Abstract. The stereodynamics of the reaction Au+H_2 have been performed by using quasi-classical trajectory (QCT) method on a global potential energy surface created by Zanchet *et al.* at the collision energy of 1.8, 2.2, 3.0 eV. The calculation on $P(\theta_r)$, $P(\phi_r)$, and $P(\theta_r,\phi_r)$ and four polarization-dependent differential cross sections (PDDCSs) in the center-of-mass (CM) indicate the dependence of the product polarization on collision energies. The product rotational angular momentum vector j' is symmetric and perpendicular to k direction according to the $P(\theta_r)$ distributions. The $P(\phi_r)$ distributions around ϕ_r=270° indicate that the rotational angular momentum vectors not only aligned along the y-axis direction, but also oriented to the y-axis negative direction. For the lower collision energy of 1.8eV, the $PDDCS_{00}$ is symmetric on the forward and backward scattering, probably due to the long lifetime complex created in the insertion reaction, while for the increasing collision energies, the prominent forward scattering is all on account of that the reaction is controlled by direct stripping.

PACS: 34.35.+a, 34.50.-s

Key words: stereodynamics, Au+H_2, quasi-classical trajectory, vector correlation.

1 Introduction

The point of view that Au is inactive as catalysts was changed by Haruta's discovery [1, 2]. Since then, Au catalysis has attracted much interest for many reactions, including low-temperature CO and alcohol oxidation [3-7], water-gas shift [8], selective hydrogenations [9-17]. This renaissance originates from the application of Au cluster catalysts which are

*Corresponding author. *Email address:* `cgmeng@dlut.edu.cn` (C. G. Meng)

prepared by innovative methods and exhibit unique reactivity different from the bulk Au catalysts.

Although the Au catalyzed hydrogenation reactions are less intensively investigated than the oxidation reaction, there are theoretical and experimental studies on the hydrogenation reactivity. Stobinski and Claus proposed that H_2 reacts and dissociates on low coordinated Au atoms at the corners or edges of the clusters [13-17]. Corma *et al.* indicated that Au atoms, which locate not only at corner or edge low coordinated positions but also not directly bonded to the supports, are active for H2 dissociation by means of periodic DF calculations [18].

The reactivity of Au cluster correlates closely with the structural and electronic properties of the cluster [19-22]. The ground atom structure $5d^{10}6s^1$ exhibits the strong relativistic effect which makes a reduced 5d-6s energy gap and strong s-d hybridization [23], as the result, the structures of Au cluster present variedly, linear (one-dimension) [19], planar (two- dimension) [24,25], and shell-like (three dimension) [26]. Recently, Zanchet *et al.* made a series of studies about structure, charge effects for the H_2 dissociation on Au cluster and obtained very interesting results [27-30]. H_2 dissociation on the linear gold chains with no barrier along the minimum energy path, and higher barriers presented on the planar clusters, however, the increased reactivity of the folded planar Au cluster is originated from the orbital flexibility when the s-d hybridization is broken. Moreover, Zanchet *et al.* established a global potential energy surface (PES) for title reaction by fitting highly correlated *Ab initio* method which is less adapted when the number of involving electrons is large. They performed quantum wave pocket and quasiclassical trajectory (QCT) calculation using the PES, and proposed that two different mechanisms control the reaction, direct and indirect. In indirect reaction mechanism, dominating at low collision energies, presence of insertion well, which is similar with the deeper chemisorption well of larger gold clusters reacting with H_2, stems from conical intersections and curve crossings with the excited electronic states Au (^{2}D) and Au (^{2}P) [28].

However, previous works mainly deal with scalar properties, vector properties representing stereodynamics of chemical reactions are not performed. The stereodynamic properties such as velocities and angular momentum with translational and rotational energies are investigated not only by magnitudes but also by well-defined directions [31-36]. Analyzing reaction dynamics together scalar with vector can provide a complete understanding on reaction dynamics. However, up to now, no literature reported the vector properties about the reaction. In order to fully understand the reaction, we investigated the three angular distributions of $P(\theta_r)$, $P(\phi_r)$, and $P(\theta_r, \phi_r)$ and four polarization-dependent differential cross sections (PDDCSs) based on the PES from Zanchet *et al.* [28].

2 Theory

2.1 Quasiclassical trajectory calculations

Calculations of the dynamical stereochemistry for the Au + $H_2 \rightarrow$ AuH + H reaction have been carried out by means of QCT method as that in refs.[31-42]. The classical Hamilton equations were numerically integrated in three dimensions. Three collision energies, 1.8, 2.2, 3.0 eV were chosen for the reaction Au + H_2, based on Zanchet's results. At 1.8 eV, just exceeding the threshold of 1.55 eV, the average lifetime of the complex is of the order of 100 fs, in contrast, the average lifetime is lower than 15fs at 3 eV. The difference of average lifetime at the two limit collision will reflect obviously in the calculations of the dynamical stereochemistry. Furthermore, The initial vibrational and rotational quantum number of the reactants were chosen as v=0 and j=0. The initial azimuthal angle and polar angle of the reagent molecule internuclear axis are randomly sampled by Monte Carlo method, and the range of the angles is from 0° to 180° and 0° to 360°, respectively. A batch of 100000 trajectories is run for each energy point and the time integration step size in the trajectories is chosen to be 0.1 fs.

2.2 Product rotational polarization

The reference frame in this work is the center-of-mass (CM) frame (as shown in Fig. 1). The z-axis is in the relative velocity direction of reagent k, and the x-z plane is scattering plane containing the reagent and product relative velocity vectors, k and k'. θ is called scattering angle between the reagent relative velocity k and the product relative velocity k'. θ_r, ϕ_r are the polar and azimuthal angles of the product rotational angular momentum j'.

The distribution function $P(\theta_r)$ describes the k-j' correlation. $P(\theta_r)$ can be expanded

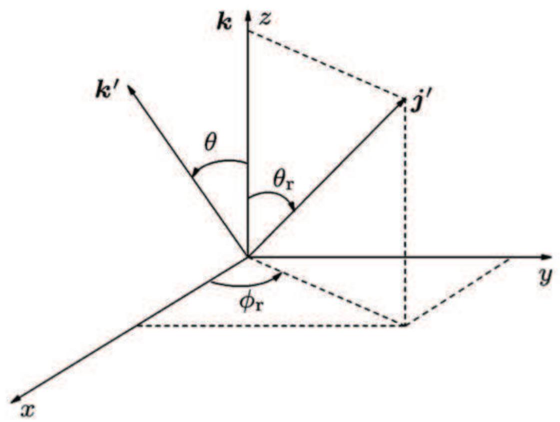

Figure 1: The center-of-mass frame used to describe k, k, and j' correlations.

into a series of Legendre polynomials as literature 34-36.

$$P(\theta_r)=\frac{1}{2}\sum_k(2k+1)a_0^{(k)}P_k(\cos\theta_r).$$

Where

$$a_0^{(k)}=\int_0^\pi P(\theta_r)P_k(\cos\theta_r)\sin\theta_r d\theta_r=\langle P_k(\cos\theta_r)\rangle.$$

The expanding coefficients are called the orientation (k is odd) or alignment (k is even) parameters. The dihedral angle distribution function $P(\phi_r)$ describing k-k'-j' correlations [36, 37], can be expanded in a series of Fourier series as

$$P(\phi_r)=\frac{1}{2\pi}\left(1+\sum_{n,even\geq 2}a_n\cos n\phi_r+\sum_{n,add\geq 1}b_n\sin n\phi_r\right).$$

Where

$$a_n=2\langle\cos n\phi_r\rangle,$$
$$b_n=2\langle\sin n\phi_r\rangle.$$

In this calculation $P(\theta_r)$ and $P(\phi_r)$ are expanded up to k=18, n=24, respectively, which thereby showing good convergence.

The joint probability density function of the angles θ_r and ϕ_r, which define the direction of j' [34], can be described as

$$P(\theta_r,\phi_r)=\frac{1}{4\pi}\sum_{kq}[k]a_q^kC_{kq}(\theta_r,\phi_r)^*=\frac{1}{4\pi}\sum_k\sum_{q\geq 0}\left[a_{q\pm}^k\cos q\phi_r-a_{q\mp}^k i\sin q\phi_r\right]C_{kq}(\theta,0).$$

The polarization parameter a_q^k is evaluated as

$$a_{q\pm}^k=2\langle C_{k|q|}(\theta_r,0)\cos q\phi_r\rangle,\quad \text{k is even},$$
$$a_{q\mp}^k=2i\langle C_{k|q|}(\theta_r,0)\sin q\phi_r\rangle,\quad \text{k is odd}.$$

In this calculation, $P(\theta_r,\phi_r)$ is expanded up to k=7, which is sufficient for good convergence.

The full three-dimensional angular distribution associated with k, k' and j' can be represented by a set of generalized polarization dependent differential cross-sections (PDDCSs) in the CM frame. The fully correlated CM angular distribution is written as the sum [31, 35, 36]:

$$P(\omega_t,\omega_r)=\sum_{kq}\frac{[k]}{4\pi}\frac{1}{\sigma}\frac{d\sigma_{kq}}{d\omega_t}C_{kq}(\theta_r,\phi_r),$$

Where $[k]=2k+1$, $1/\sigma(d\sigma_{kq}/d\omega_t)$ is a generalized polarization dependent differential cross-sections (PDDCSs), $C_{kq}(\theta_r,\phi_r)$ are modified spherical harmonics. The angles $\omega_t=$

θ_t,ϕ_t and $\omega_r{=}\theta_r,\phi_r$ refer to the coordinates of the unit vectors k' and j' along the directions of the product relative velocity and rotational angular momentum vectors in the CM frame, respectively [40].

$1/\sigma(d\sigma_{kq}/d\omega_t)$ yields [31]:

$$\frac{1}{\sigma}\frac{d\sigma_{k0}}{d\omega_t}=0 \quad (k \text{ is odd}),$$

$$\frac{1}{\sigma}\frac{d\sigma_{kq+}}{d\omega_t}=\frac{1}{\sigma}\frac{d\sigma_{kq}}{d\omega_t}+\frac{1}{\sigma}\frac{d\sigma_{k-q}}{d\omega_t}=0 \quad (k \text{ even, and } q \text{ even or } k \text{ odd, and } q \text{ even}),$$

$$\frac{1}{\sigma}\frac{d\sigma_{kq-}}{d\omega_t}=\frac{1}{\sigma}\frac{d\sigma_{kq}}{d\omega_t}-\frac{1}{\sigma}\frac{d\sigma_{k-q}}{d\omega_t}=0 \quad (k \text{ even, and } q \text{ odd or } k \text{ odd, and } q \text{ odd}).$$

In this work, $(2\pi/\sigma)(d\sigma_{20}/d\omega_t)$, $(2\pi/\sigma)(d\sigma_{00}/d\omega_t)$, $(2\pi/\sigma)(d\sigma_{22+}/d\omega_t)$ and $(2\pi/\sigma)(d\sigma_{21-}/d\omega_t)$ named PDDCS$_{00}$, PDDCS$_{20}$, PDDCS$_{22+}$ and PDDCS$_{21-}$ are calculated.

3 Results and discussion

In order to obain a abundant information of polarization of the reaction, we plotted the $P(\theta_r)$ distributions at collision energy of 1.8, 2.2, 3.0 eV as shown in Fig. 2, which described the k-j' correlation. Under three condition of collision energies, the peaks of the $P(\theta_r)$ distribution are at θ_r=90° and symmetric with respect to 90°, which presents that the product rotational angular momentum vector j' is symmetric and perpendicular to k direction. Furthermore, as the collision energies increase, the peaks of $P(\theta_r)$ become sharper and stronger, indicating angular momentum polarization becomes more prominent. The investigation on the potential energy surface of Au + H_2 reaction indicated that

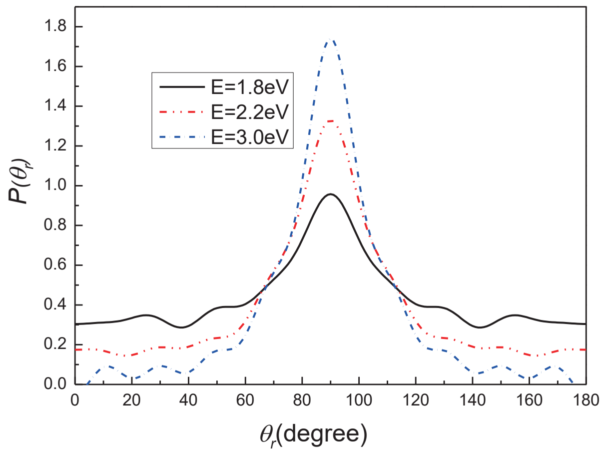

Figure 2: A comparison of $P(\theta_r)$ distribution at different collision energy 1.8, 2.2 and 3.0eV for the reaction of Au + H_2(v=0, j=0) → AuH + H.

there are two different reaction paths from reactants to products by Zanchet *et al.* [28]. The presence of potential well decides the existence of long-lived complex at low energies. Longer lifetime leads to the losing of "memory" for the direction of initial angular momentum, which weakened the rotational polarization of products.

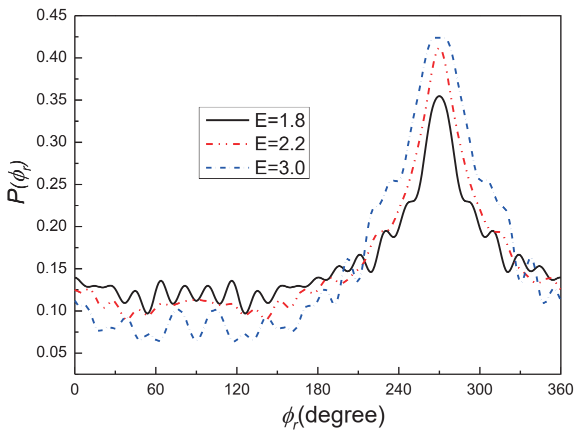

Figure 3: A comparison of $P(\phi_r)$ distribution at different collision energies 1.8, 2.2 and 3.0eV for the reaction of Au + H_2 (v=0, j=0) → AuH + H.

The dihedral angle distributions $P(\phi_r)$ as shown in Fig. 3 characterize k-k'-j' three vector correlation, and provide the stereodynamical information for the alignment and orientation of products. It can be seen that the $P(\phi_r)$ tends to be asymmetric with respect to the k-k' scattering plane (at about ϕ_r=180°), the peak at ϕ_r=270° implies that the rotational angular momentum vectors not only aligned along the y-axis direction, but also oriented to the y-axis negative direction, i.e. the products left-handed rotate mainly parallel to the scattering plane. When the collision energies increase, the peaks at ϕ_r=270° become broader and higher, which indicates the rotations of the products have tendency from in-plane reaction mechanism to out-plane reaction mechanism. The more obvious pictures on rotational polarization of the product in three dimensions are obtained by the distribution $P(\theta_r,\phi_r)$ as shown in Fig. 4. The peaks at (90°, 270°) are in good accordance with the distribution $P(\theta_r)$ and $P(\phi_r)$. The results from Fig. 4 confirm that the products are preferentially polarized perpendicular to the scattering plane and the reaction is dominated by the in-plane mechanism.

The polarization-dependent differential cross-sections (PDDCSs) enrich polarization information of product angular momentum. Fig. 5 presents PDDCS_{00}, PDDCS_{20}, PDDCS_{22+} and PDDCS_{21-} in the title reaction. PDDCS_{00} describes the product angular distribution, simply proportional to the differential cross section (DCS). These results of PDDCS_{00} are accordant with Zanchet A' reports on DCS in the title reaction [28]. There are two different reaction mechanisms: direct and indirect according to different collision energy. For the lower collision energy considered, 1.8eV, just exceeding the threshold of energy

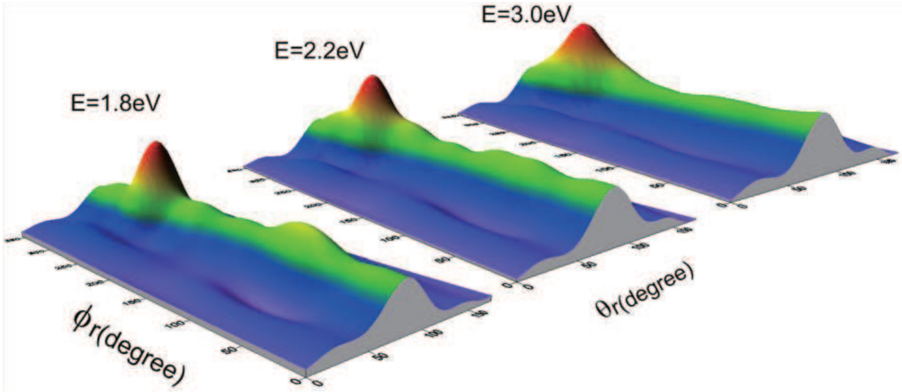

Figure 4: 3D plots of $P(\theta_r,\phi_r)$ distribution averaged over all scattering angles for the reaction of Au + H_2 (v=0, j=0) → AuH + H at the collision energies 1.8, 2.2 and 3.0eV.

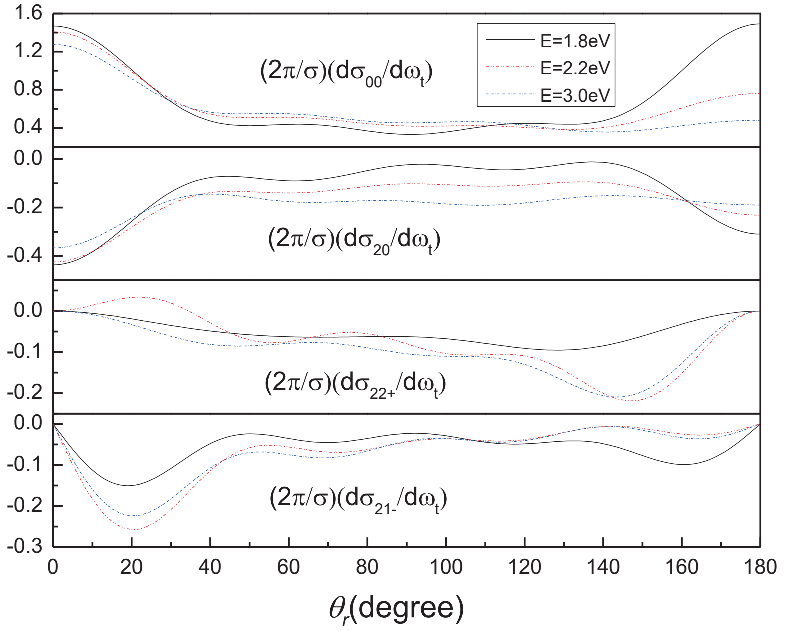

Figure 5: PDDCS: $(2\pi/\sigma)(d\sigma_{00}/d\omega_t)$, $(2\pi/\sigma)(d\sigma_{20}/d\omega_t)$, $(2\pi/\sigma)(d\sigma_{22+}/d\omega_t)$ and $(2\pi/\sigma)(d\sigma_{21-}/d\omega_t)$ for the reaction of Au + H_2 (v=0, j=0) → AuH + H at three different collision energies 1.8, 2.2 and 3.0eV.

at 1.7eV, $PDDCS_{00}$ shows the forward and backward scattering, almost symmetric, the isotropy may come from the long lifetime complex in the insertion reaction. However, as the collision energies increase, the forward scattering directions are more obvious, and reactions may be controlled by the direct stripping mechanism. $PDDCS_{20}$ is the expectation value of the second Legendre moment, presents the alignment of product in the range of scattering angular distribution. The negative value implies that j' is aligned perpendicular to k, and the larger absolute value, the more distinct the alignment trend. In the extreme scattering directions of forward and backward, PDDCS_{22+} and PDDCS_{21-} (q≠0) are equal to zero, (as shown in Figs. 5(c) and (d)), which is due to that the k-k' scattering plane are uncertain in the restricted scattering directions. In contrast, the PDDCS_{22+} and PDDCS_{21-} basically below zero indicate the distributions $P(\theta_r,\phi_r)$ are anisotropic at scattering angles away from the extreme direction.

4 Conclusion

The stereodynamics for the reaction Au + H_2 (v=0, j=0) $\rightarrow$ AuH + H have been investigated by using quasi-classical trajectory methods at collision energy of 1.8, 2.2, 3.0 eV. Three angular momentum distributions of $P(\theta_r)$, $P(\phi_r)$, and $P(\theta_r,\phi_r)$ and four polarization-dependent differential cross sections (PDDCSs) are calculated. The product rotational angular momentum vector j' is symmetric and perpendicular to k direction according to the $P(\theta_r)$ distributions. The $P(\phi_r)$ distributions around ϕ_r=270° indicate that the rotational angular momentum vectors not only aligned along the y-axis direction, but also oriented to the y-axis negative direction. For the lower collision energy of 1.8eV, the PDDCS_{00} is symmetric on the forward and backward scattering, probably due to the long lifetime complex created in the insertion reaction, while for the increasing collision energies, the prominent forward scattering is all on account of that the reaction is controlled by direct stripping, which is in accordance with the Zanchet's results.

Acknowledgments. This work was supported by the National Natural Science Foundation of China (Grant No. 21271037).

References

[1] M. Haruta, T. Kobayashi, H. Sano, Chem. Lett. 2 (1987) 405.
[2] M. Haruta; N. Yamada; T. Kobayashi; S. Iijima, J. Catal. 115 (1989) 301.
[3] M. Haruta, Catal. Today 36 (1997) 153.
[4] M. Valden, X. Lai, D. W. Goodman, Science 281 (1998) 1647.
[5] J. Guzman, S. Carrettin, A. Corma, J. Am. Chem. Soc. 127 (2005) 3286.
[6] G. J. Hutchings, Gold Bull. 37 (2004) 3.
[7] A. Abad, P. Concepcion, A. Corma, H. Garcia, Angew. Chem. Int. Ed. 44 (2005) 4066.
[8] Q. Fu, H. Saltsburg, M. Flytzani-Stephanopoulos, Science 301 (2003) 935.
[9] J. Jia, K. Haraki, J. N. Kondo, K. Domen, J. Phys. Chem. B 104 (2000) 11153.
[10] J. E. Bailie, G. J. Hutchings, Chem. Commun. 21 (1999) 2151.
[11] A. Corma, P. Serna, Science 313 (2006) 332.
[12] N. Weiher, A. M. Beesley, N. Tsapatsaris, L. Delannoy, C. Louis, J. A. van Bokhoven, S. L. M. Schroeder, J. Am. Chem. Soc. 129 (2007) 2240.
[13] P. Claus, Appl. Catal. A. General 291 (2005) 222.
[14] L. Stobinski, R. Nowakowski, R. Dus, Vaccum 48 (1997) 203.
[15] L. Stobinski, L. Zommer, R. Dus, Appl. Surf. Sci. 141 (1999) 319.
[16] L.Stobinski, R. Dus, Appl. Surf. Sci. 62 (1992) 77.

[17] L. Stobinski, Appl. Surf. Sci. 103 (1996) 503.
[18] M. Boronat, F. Illas, and A. Corma, J. Phys. Chem. A 113 (2009) 3750.
[19] H. Häkkinen, R. N. Barnett, U. Landman, J. Phys. Chem. B 103 (1999) 8814.
[20] S. Gilb, P. Weis, F. Furche, R. Ahlrichs, J. Chem. Phys.116 (2002) 4094.
[21] A. Lechtken, C. Neiss, M. M. Kappes, D. Schooss, Phys. Chem. Chem.Phys.11 (2009) 4344.
[22] R. B. King, Z. Chen, P. V. Schleyer, Inorg. Chem. 43 (2004) 4564.
[23] H. Häkkinen, M. Moseler, U. Landman, Phys. Rev. Lett.89 (2002) 033401.
[24] H. Häkkinen, S. Abbet, A. Sanshez, U. Heiz, U. Landman, Angew. Chem. Int. Ed. 42 (2003) 1297.
[25] H. M. Lee, M. Ge, B. R. Sahu, P. Tarakeshwar, K. S. Kim, J. Phys. Chem. B 107 (2003) 9994.
[26] F. Furche, R. Ahlrichs, P. Weis, C. Jacob, S. Gilb, T. Bierweiler, M. M. Kappes, J. Chem. Phys. 117 (2002) 6982.
[27] A. Zanchet, A. Dorta-Urra, O. Roncero, F. Flores, C. Tablero, M. Paniagua, A. Aguado, Phys. Chem. Chem. Phys. 11 (2009) 10122.
[28] A. Zanchet, O. Roncero, S. Omar, M. Paniagua, A. Aguado, J. Chem. Phys. 132 (2010) 034301.
[29] A. Zanchet, A. Dorta-Urra, A. Aguado, O. Roncero, J. Phys. Chem. C 115 (2011) 47.
[30] A. Dorta-Urra, A. Zanchet, O. Roncero, A. Aguado, J. Chem. Phys. 135 (2011) 091102.
[31] N. E. Shafer-Ray, A. J. Orr-Ewing, R. N. Zare, J. Chem. Phys. 99 (1995) 7591.
[32] K. S. Bradley, G. C. Schatz, J. Chem. Phys. 106 (1997) 8464.
[33] U. Fano, J. H. Macek, Rev. Mod. Phys. 45 (1973) 553.
[34] F. J. Aoiz, M. Brouard, P. A. Enriquez, J. Chem. Phys. 105 (1996) 4964.
[35] M. Brouard, H. M. Lambert, S. P. Rayner, J. P. Simons, Mol. Phys. 89 (1996) 403.
[36] A. J. Orr-Ewing, R. N. Zare, Ann. Rev. Phys. Chem. 45 (1994) 315.
[37] M. P. deMiranda, D. C. Clary, J. F. Castillo, D. E. Manolopoulos, J. Chem. Phys. 108 (1998) 3142.
[38] M. P. deMiranda, D. C. Clary, J. Chem. Phys. 106 (1997) 4509.
[39] M. D. Chen, K. L. Han, N. Q. Lou, Chem. Phys. 283 (2002) 463.
[40] M. D. Chen, K. L. Han, N. Q. Lou, Chem. Phys. Lett. 357 (2002) 483.
[41] M. L. Wang, K. L. Han, G. Z. He, J. Chem. Phys. 109 (1998) 5446.
[42] K. L. Han, G. Z. He, N. Q. Lou, J. Chem. Phys. 105 (1996) 8699.